Optimization of Biomass, Vitamins, and Carotenoid Yield on Light Energy in a Flat-Panel Reactor Using the A-Stat Technique

Maria J. Barbosa,[1] Jan Willem Zijffers,[1] Adrian Nisworo,[1] Woulter Vaes,[2] Jan van Schoonhoven,[2] René H. Wijffels[1]

[1]Food and Bioprocess Engineering Group, Wageningen University, P.O. Box 8129, 6700 EV Wageningen, The Netherlands; telephone: +31-317-483396; fax: +31-17-482237; e-mail: maria.barbosa@wur.nl
[2]Department of Food and Food Supplement Analysis, TNO Nutrition and Food Research, Zeist, The Netherlands

Received 21 February 2003; accepted 10 September 2004

Published online 8 December 2004 in Wiley InterScience (www.interscience.wiley.com). DOI: 10.1002/bit.20346

Abstract: Acceleration-stat (A-stat) cultivations in which the dilution rate is continuously changed at a constant acceleration rate, leading to different average light intensities inside the photobioreactor, can supply more information and reduce experimental time compared with chemostat cultivations. The A-stat was used to optimize the biomass and product yield of continuous cultures of the microalgae *D. tertiolecta* in a flat-panel reactor. In this study, four different accelerations were studied, a pseudo steady state was maintained at acceleration rates of 0.00016 and 0.00029 h^{-2} and results were similar to those of the chemostat. An increase in the acceleration rate led to an increase in the deviation between results obtained in the A-stat and in the chemostats. We concluded that it is advantageous to use the A-stat instead of chemostats to determine culture characteristics and optimize a specific photobioreactor. The effect of average light intensity inside the photobioreactor on the production of vitamins C and E, lutein, and β-carotene was studied using the A-stat. The highest concentrations of these products were 3.48 ± 0.46, 0.33 ± 0.06, 5.65 ± 0.24, and 2.36 ± 0.38 mg g^{-1}, respectively. These results were obtained at different average light intensities, showing the importance of optimizing each product on light intensity.

Keywords: microalgae; A-stat; flat-panel; vitamins; carotenoids; light

INTRODUCTION

Microalgae are a natural source of specific and attractive compounds for the pharmaceutical cosmetic and food industry. The efficiency of microalgal cultivation systems can be characterized by volumetric productivity and efficiency of light utilization. In photobioreactors, light energy is the growth-limiting substrate and should be used efficiently for growth and production of the desired compounds. Optimization of biomass and product yields on light energy is thus essential for cost-effective photobioreactors.

Steady-state culture characteristics are generally used to study growth and production kinetics as well as physiological characteristics of microorganisms. Usually, these characteristics are determined in chemostat cultivations, which are time-consuming because a large number of steady-state points are necessary. In acceleration-stat (A-stat) cultivations, a cultivation parameter is changed continuously with a constant acceleration rate, and therefore it requires less time to study a wider range of steady states (Paalme et al., 1995). It is essential to find a compromise between the highest acceleration rate (i.e., the fastest A-stat) and an acceptable approximation of steady-state conditions (Sluis et al., 2001).

This technique was previously used with the microalgae *Dunaliella tertiolecta* grown in a pilot-plant bubble column, by continuously changing the dilution rate at a constant rate. It was shown that the A-stat was accurate and fast for optimizing productivity of a continuous culture of *D. tertiolecta* (Barbosa et al. 2003).

In the present work we studied the applicability of this technique to optimize product and biomass yield on light energy in a flat-panel photobioreactor with a differing light regimen.

D. tertiolecta is one of the few organisms that simultaneously produces antioxidant vitamins such as carotenoids (β-carotene, lutein), vitamin C (ascorbic acid), and vitamin E (α-tocopherol) (Abalde and Fabregas, 1991; Takeyama et al., 1997). The antioxidant properties of these molecules have received much attention due to their application in the clinical and nutritional fields (Takeyama et al., 1997).

Correspondence to: M.J. Barbosa
Contract grant sponsor: Fundação para a Ciência e Tecnologia
Contract grant number: PRAXIS XXI/BD/19539/99

The production of these molecules by microalgae cells is dependent on the light intensity (main substrate in phototrophic cultivations) (Abe et al., 1999; Kusmic et al., 1999; Phillips et al., 1995). However, the effect of a wide range of light intensities and light regimes on the production of these products in continuous cultivations of *D. tertiolecta* has never been studied.

For the aforementioned reasons, vitamin C, vitamin E, lutein, and β-carotenoid yield on light energy were optimized using the A-stat technique.

MATERIALS AND METHODS

Strain and Culture Medium

Dunaliella tertiolecta CCAP 19/6B was obtained from the Culture Collection of Algae and Protozoa (Oban, UK) and maintained as a pure suspended culture, as described elsewhere (Barbosa et al., 2003). The reactor was inoculated with 100 mL of pure inoculum.

Cultivation System

The A-stats were carried out in a flat-panel built up from lexan (polycarbonate) plates held together in a stainless-steel frame, with a height, diameter, and depth of 0.60, 0.2, and 0.03 m (Fig. 1), respectively, and a culture volume of 3.4 L.

The reactor was illuminated continuously at one surface by 10 fluorescent tubes (Lynx LE, Sylvania) and the incident light intensity was approximately 1000 μmol m^{-2} s^{-1} for each experiment.

During all cultivations, a Bio-controller (Applikon, The Netherlands) controlled the cultivation parameters (pH and temperature) and the BIOXPERT program (Applikon) obtained the on-line data, which included temperature, pH, medium flow rate, air and carbon dioxide flow rate, and weight of the medium vessel. The medium was pumped by a tube pump (Model 205U, Watson-Marlow), which was controlled by the BIOXPERT program. Due to possible alterations of the pump tube over time, the real medium flow rate was calculated at the end of each experiment as the decrease in weight of the medium vessel in time, which was monitored with a balance (BP 34000-P, Sartorius) that was also connected to the BIOXPERT program. The reactor was equipped with a water jacket (Fig. 1) connected to a cryostat, which controlled the temperature at 30°C. The pH was controlled at 7.8 by adding carbon dioxide to the air flow and the gas flow rate was 3.0 L min^{-1}. The air was sparged through 17 needles with a diameter of 0.8 mm and a length of 40 mm. The needles were pinched through a piece of silicon positioned at the bottom of the reactor.

Cultivations

Before each experiment, the cultivation ran batchwise until the biomass concentration was approximately 2.5 g L^{-1}, then a constant dilution rate was started. This dilution rate was kept constant for three residence times to reach steady state. Steady-state conditions were ascertained by constant biomass concentration, constant ratio OD_{680}/OD_{530}, which was measured daily, and a constant carbon dioxide supply, which was measured online during all cultivation times and was used to control pH. This was performed for both chemostat and A-stat experiments (Fig. 2a).

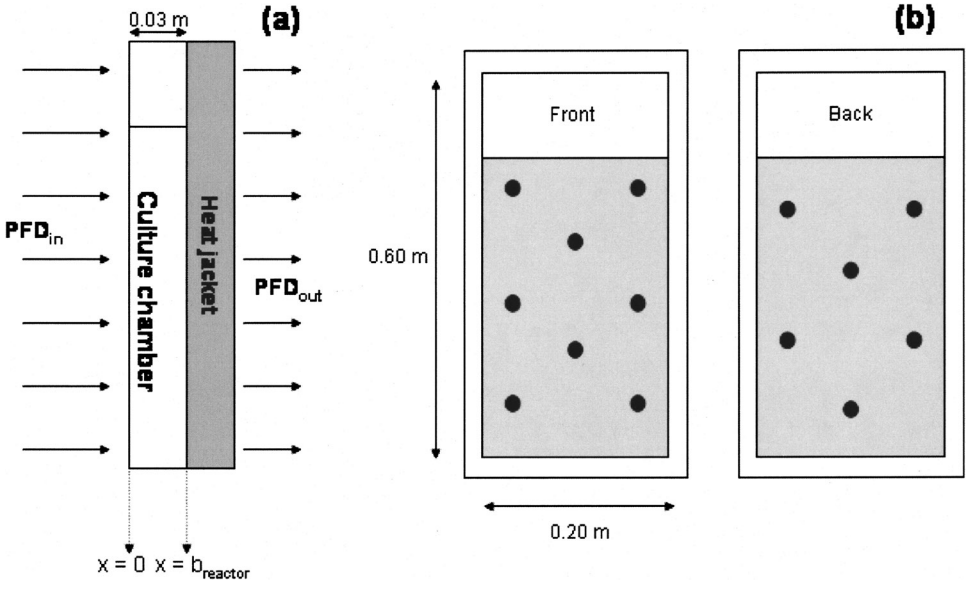

Figure 1. Scheme of the flat-panel reactor: (a) side view and (b) front view. Filled circles represent measuring points for light intensity in the back and in the front (illuminated surface) of the reactor.

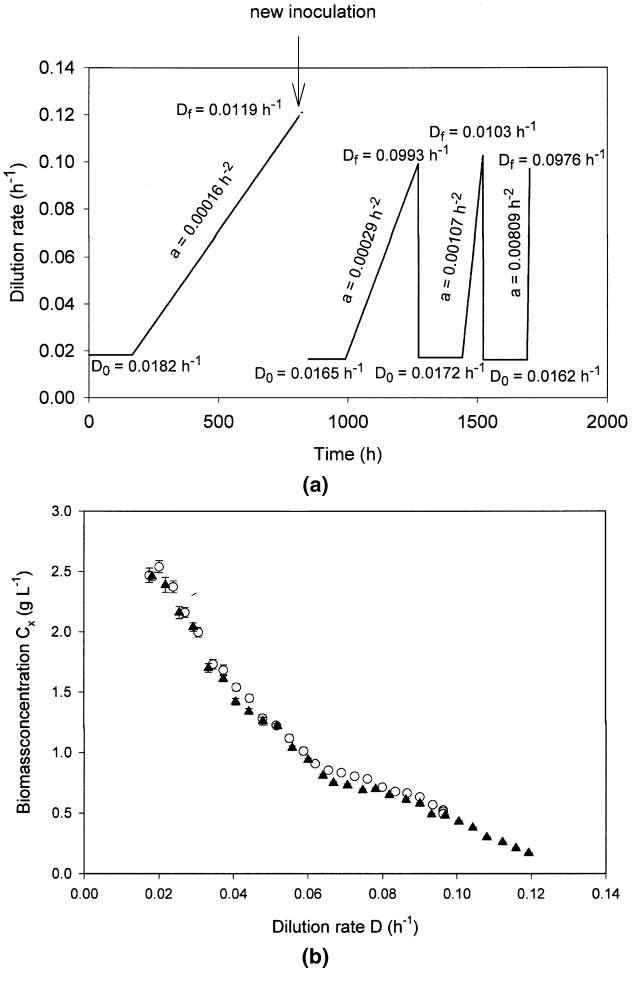

Figure 2. (a) Scheme of the dilution rate during the experiments conducted to study the effect of acceleration rate on pseudo-steady-state culture characteristics. D_0, initial dilution rates; D_f, final dilution rates; a, acceleration rate. (b) Experimental biomass concentrations (C_x) during the A-stat, performed at an acceleration rate of 0.00016 h^{-2} (▲) and 0.00015 h^{-2} (○).

A-Stats

After steady state was reached during chemostat, a smooth, constant increase in dilution rate (D) was started, according to:

$$D = D_0 + a \cdot t \qquad (1)$$

Four acceleration rates (a) were studied, 0.00016, 0.00029, 0.00107, and 0.00809 h^{-2}, which corresponded to A-stat cultivation times of 27.4, 11.8, 3.35, and 0.48 days, respectively. A scheme of the experiments performed over time, with the values for the initial and final dilution rates for each A-stat, is shown in Figure 2a.

The first A-stat ran until washout of the cells. For this reason a new inoculation was made before starting the other experiments (Fig. 2a).

A duplicate of the first A-stat was performed to optimize product yield. Due to practical reasons (tubing deformation in time during cultivation), the acceleration rate was slightly lower, 0.00015 instead of 0.00016 h^{-2}.

A-Stat Reproducibility

To optimize biomass and product yield on light energy and to verify the reproducibility of the A-stat, a duplicate of the first A-stat (a = 0.00016 h^{-2}) was performed by continuously changing the dilution rate from 0.0175 up to 0.0963 h^{-1}. Due to practical reasons (tubing deformation during cultivation), the acceleration rate (measured at the end of the experiment with the on-line measurements of the weight of the medium vessel) was slightly lower than in the first A-stat, 0.00015 instead of 0.00016 h^{-2} (Fig. 2b). The choice of acceleration rate was based on the previous A-stat carried out at this acceleration rate, which led to pseudo-steady-state conditions (Fig. 3a) and to the similarity of data obtained by chemostat at the same dilution rate (Fig. 5). Despite the small change in acceleration rate, the results of both A-stats were very similar, showing the reproducibility of the technique (Fig. 2b).

Chemostats

Three different chemostats were carried out at three different dilution rates, 0.0455, 0.0603, and 0.1016 h^{-1}, under the same conditions as during the A-stat.

Photon Flux Density

The photon flux density (PFD) was measured as photosynthetic active radiation (PAR), 400 to 700 nm, with a 2 PAR sensor (LI-190SA, LI-Cor, Lincoln, NE). The PFD falling on the reactor surface (PFD_{in}) was measured at the beginning and at the end of each experiment to verify whether the PFD_{in} was constant during the cultivation time. The PFD_{in} is the average of different measurements at eight different locations of the illuminated area (Fig. 1).

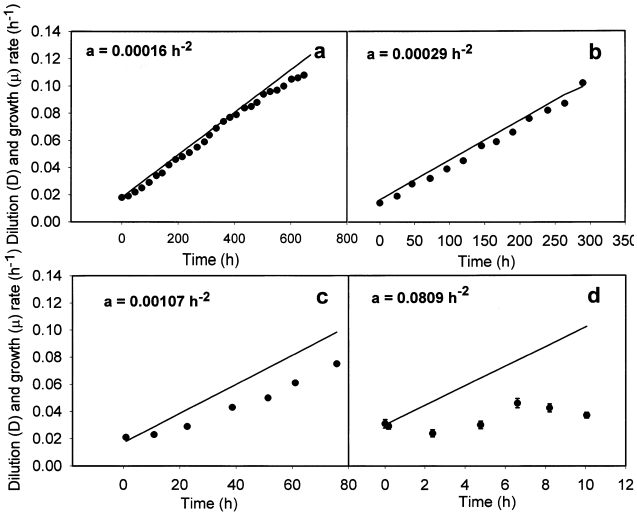

Figure 3. Effect of acceleration rate (a) on pseudo steady state during the A-stat cultivation of *D. tertiolecta*. (a) 0.00016 h^{-2}, (b) 0.00029 h^{-2}, (c) 0.00107 h^{-2}, and (d) 0.00809 h^{-2}. Solid line indicate dilution rate; discrete points indicate growth rate. Error bars represent standard errors.

The PFD coming through the reactor was measured daily at the back of the reactor during cultivation (PFD_{out}). The PFD_{out} is the average of measurements at six different locations (Fig. 1).

Sample Standardization

Culture samples were collected on a daily basis. The optical density was measured at 680 nm ($OD_{680,sample}$) and the volume of culture suspension (V_{sample}) required for further analysis was calculated according to:

$$V_{sample} = V_{standard} \cdot \frac{OD_{680,standard}}{OD_{680,sample}} \quad (2)$$

where $V_{standard}$ is the necessary culture volume with a certain optical density ($OD_{680,standard}$) to perform the analysis. After choosing an $OD_{680,standard}$, which was arbitrarily chosen to be 1.4, $V_{standard}$ can be determined.

The suspension collected from the reactor was centrifuged at 5000*g*, 4°C, for 5 min (Beckman J2-MC centrifuge with a JA-20 rotor). The supernatant was centrifuged again. Both pellets were resuspended in a certain volume ($V_{standard}$) of ASW (depending on which analysis is to be done) to a final optical density of $OD_{680,standard}$ = 1.4. This washed suspension was used for determination of dry weight, protein, chlorophyll, and average spectral absorption coefficient.

Vitamins and Carotenoids

The principle used to standardize the sample was also used to prepare the sample to be analyzed for vitamin and carotenoid content. For determination of vitamin content, a total volume of $V_{standard}$ = 65 mL with an $OD_{680,standard}$ = 2 was needed. The sample volume (V_{sample}) needed to be collected was calculated using Eq. (2).

This sample was centrifuged twice, using the same conditions as mentioned earlier, and the pellets were resuspended in 65 mL of a solution of 0.01% (w/v) sodium erythorbate (isoascorbic acid) in 0.5 *M* ammonium formate.

Two tubes were filled with 30 mL of the resuspended algae and were centrifuged again under the same conditions. The supernatant was discarded and the pellets were frozen at −20°C until vitamin and carotenoid analysis.

Analysis

Dry weight, chlorophyll, optical density, and spectral absorption coefficient per dry weight were determined as previously described (Barbosa et al., 2003).

Vitamins and Carotenoids

Vitamin C. Vitamin C was analyzed according to Speek et al. (1984). Samples were extracted using 5% trichloroacetic acid. The extract obtained was adjusted to pH 4.5, after which ascorbic acid was enzymatically oxidized by ascorbate oxidase to dehydroascorbic acid. Dehydroascobic acid was derivatized by 12-diamonibenzene to its quinoxaline derivative, which was analyzed using reverse-phase high-performance liquid chromatography (HPLC) with fluorescence detection (excitation λ 355 nm, emission λ 425 nm).

Carotenoids and Tocopherols

Samples were saponified during 30 min at 80°C by ethanolic KOH (10%) containing 2% sodium ascorbate. After cooling to room temperature, the mixture was extracted by isopropylether. The extract was dried under a gentle flow of nitrogen, and the residue dissolved in hexane. Subsequently, the samples were analyzed for tocopherols using straight-phase HPLC with fluorescence detection (excitation λ 296 nm, emission λ 320 nm), as described by Speek et al. (1985), and for carotenoids using reverse-phase HPLC with photodiode array (PDA) detection, as described by Broekmans et al. (2002).

Calculations

Growth Rate

As the dilution rate (D) varied linearly during the A-stat and the volume (V) remained constant, the specific growth rate was derived from the experimental biomass concentration. At each experimental timepoint (t), the specific growth rate was calculated by averaging the growth rate at time t_{t-1} and t_{t+1}, according to:

$$u_t = \frac{\frac{C_{x,t}-C_{x,t-1}}{(t_t-t_{t-1})\cdot C_{x,t}} + \frac{C_{x,t}-C_{x,t+1}}{(t_t-t_{t+1})\cdot C_{x,t}} + 2 \cdot D_t}{2} \quad (3)$$

where $C_{x,t}$, $C_{x,t-1}$, and $C_{x,t+1}$ are the biomass concentrations at time t_t, t_{t-1}, and t_{t+1}, respectively.

Average Light Intensity

The average light intensity (PFD_{ave}) and the light gradient inside the reactor were calculated using Beer's law:

$$PFD_{out}(\lambda) = PFD_{in}(\lambda) \cdot e^{-a_c(\lambda)\cdot C_x \cdot b} \quad (4)$$

The average wavelength-dependent light intensity ($PFD_{ave}[\lambda]$) inside the reactor was determined by integrating Eq. (5) between $x = 0$ and $x = b_{reactor}$ (Fig. 1):

$$PFD_{ave}(\lambda) = \frac{\int_0^{b_{reactor}} PFD_{in}(\lambda) \cdot e^{-a_c(\lambda)\cdot C_x \cdot x dx}}{\int_0^{b_{reactor}} 1 \cdot dx} \quad (5)$$

The solution to this integral is given by:

$$\mathrm{PFD_{ave}}(\lambda) = \mathrm{PFD_{in}}(\lambda) \cdot \frac{1}{b_{\mathrm{reactor}}}(1 - e^{-a_c(\lambda)\cdot C_x \cdot b_{\mathrm{reactor}}}) \cdot \frac{1}{C_x \cdot a_x(\lambda)} \quad (6)$$

and the average light intensity ($\mathrm{PFD_{ave}}$) calculated as follows:

$$\mathrm{PFD_{ave}} = \sum_{400}^{700} \mathrm{PFD_{ave}}(\lambda) \cdot \Delta\lambda \quad (7)$$

Eq. (7) was solved numerically by taking small steps of 0.5 nm (measurement step of the absorption of the sample and of the spectrum of the lamp), between 400 and 700 nm, which corresponds to the PAR range.

Light Gradient and Light Penetration Depth

The light gradient was calculated by Eq. (4), by replacing the light path (b) for different reactor depths.

The photic volume in the photobioreactor was calculated based on the light gradient and was arbitrarily defined as the reactor depth at which 90% of the incoming light intensity is absorbed (Janssen et al., 2002; Richmond and Cheng-Wu, 2001).

Biomass and Product Yield on Light Energy

The biomass yield on light energy ($Y_{x,E}$) was calculated according to:

$$Y_{x,E} = \frac{P_x \cdot V_{\mathrm{reactor}}}{E_a \cdot 10^{-6} \cdot 3600} \quad (8)$$

where P_x is the biomass volumetric productivity ($\mathrm{g\,L^{-1}\,h^{-1}}$), the value 3600 is used to convert seconds to hours, V_{reactor} is the reactor volume (L), E_a is the amount of light absorbed (μmol photons $\mathrm{s^{-1}}$), and 10^{-6} is used to convert micromoles to moles of photons. The product yield on light energy was calculated by using the same equation, replacing the biomass volumetric productivity with the product volumetric productivity.

Light Absorbed

The amount of light energy absorbed was calculated by subtracting the measured $\mathrm{PFD_{out}}$ (corrected by the water jacket, Fig. 1) to the measured light intensity falling on the reactor surface ($\mathrm{PFD_{in}}$).

RESULTS AND DISCUSSION

Effect of Acceleration Rate on Pseudo-Steady-State Conditions

The choice of acceleration rate during an A-stat cultivation is important to keep the system at a pseudo steady state. The acceleration rate should be fast enough to reduce experimental time but it should also be slow enough to allow the microorganism to adapt its metabolism to the new conditions imposed by the change in dilution rate.

A-stats with different acceleration rates and chemostats at fixed dilution rates were performed (Fig. 2a). During the A-stats, the dilution rate increased from ca. 0.017 to 0.100 $\mathrm{h^{-1}}$. At the lowest acceleration rate (a = 0.00016 $\mathrm{h^{-2}}$), the A-stat was run until washout of the culture to determine the maximum growth rate ($\mu_{\max}$ = 0.11 $\mathrm{h^{-1}}$). At beyond a dilution rate of 0.10 $\mathrm{h^{-1}}$, the difference between dilution and growth rate increased (Fig. 3a).

The specific growth rate (μ) was derived from the experimental biomass concentration [Eq. (3)] and is depicted in Figure 3 with the dilution rate, as a function of time. It can be seen that an increase in acceleration rate resulted in an increased deviation between growth and dilution rate. The largest difference between the dilution rate imposed and the growth rate calculated increased from 15% to 76% with increasing acceleration rate from 0.00016 to 0.00809 $\mathrm{h^{-2}}$.

At the two lowest acceleration rates, 0.00016 (27.4 days) and 0.00029 $\mathrm{h^{-2}}$ (11.8 days), the growth rate was always greater than 85% and 78% of the dilution rate, respectively. We concluded that a pseudo steady state was maintained throughout the entire range of dilution rates at these acceleration rates. At an acceleration of 0.00107 $\mathrm{h^{-2}}$ (3.3 days) the growth rate dropped until 70% of the dilution rate. With the fastest A-stat (a = 0.00809 $\mathrm{h^{-2}}$; 0.42 day) the growth rate clearly could not keep up with the dilution rate (Fig. 3d) and remained almost constant. The acceleration rate should be a compromise between the required accuracy of the results and the experimental time; therefore, it may vary for different experiments with different aims.

Effect of Acceleration Rate on Culture Characteristics

Increasing the dilution rate led to a decrease of biomass concentration, as shown in Figure 4. The steepness of the biomass decrease is strongly dependent on the acceleration rate. In the fastest A-stat (a = 0.0809 $\mathrm{h^{-2}}$), there was a very small decrease in biomass concentration when compared with the other A-stats.

During these microalgae cultivations, light is the limiting substrate. An increase in dilution rate would lead directly to a decrease in biomass concentration, which results in a higher average light intensity inside the reactor, although the dilution rate itself does not have a direct effect on the light intensity.

If we consider a constant biomass concentration inside the reactor (no growth and no death), with behavior similar to a substrate, we can simulate the effect of rate of change of

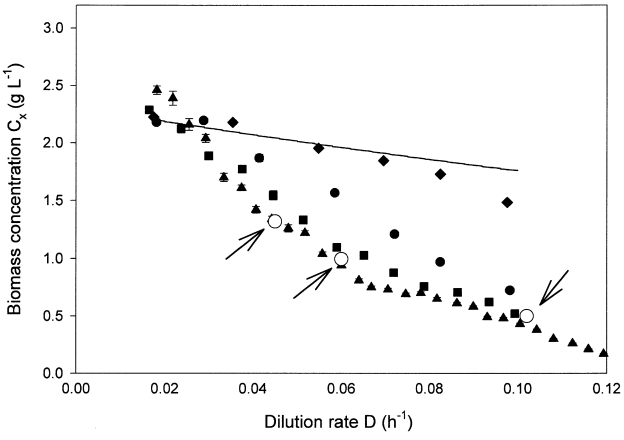

Figure 4. (a) Effect of acceleration rates of 0.00809 h^{-2} (◆), 0.00107 h^{-2} (●), 0.00029 h^{-2} (■), and 0.00016 h^{-2} (▲) during A-stat cultivations on biomass concentration and comparison to chemostat experiments (○) performed at three different dilution rates. Simulation of an acceleration rate of 0.00809 h^{-2} (solid line) using Eq. (9). Error bars represent standard errors for the A-stat data and 95% confidence interval for the chemostat data points.

dilution rate on biomass concentration during A-stats using a mass balance [Eq. (9)]:

$$\frac{dC_x}{dt} = -(D_0 + a \cdot t) \cdot C_x \qquad (9)$$

The calculated biomass concentrations, assuming that growth and death are neglected during A-stat cultivation at the fastest acceleration rate (0.00809 h^{-2}), are compared in Figure 4.

There is a delay in the decrease of biomass concentration at high acceleration rates. If there are no changes in biomass concentration, there will be no changes in average light inside the reactor and, consequently, the growth rate will also remain constant (Figs. 3d and 5a).

The average light intensity inside the reactor is directly dependent on the cell concentration and on light-dependent physiological characteristics, such as light absorption coefficient and chlorophyll content. The cells have the capacity to adapt their photosynthetic apparatus to different light intensities in a process called photoacclimation. When cultivated under a certain light intensity, cells exhibit a corresponding size of the cellular light-absorbing surface, consisting of pigment molecules arranged in antenna complexes inside the photosystem. The specific surface, that is, the absorption coefficient, decreases if the light intensity increases (Falkowski and LaRoche, 1991).

The average light intensity was calculated based on Beer's law [Eq. (5)], which is based only on light absorption. Especially at high biomass concentrations, light scattering by microalgae increases the light path, and the probability of absorption should increase. In fact, the average light intensity is smaller than the values presented in Figure 5a.

In Figure 5b and c, a decreases of both absorption coefficient and chlorophyll content were observed with increasing average light intensity, except at the highest acceleration rate, where it remained constant.

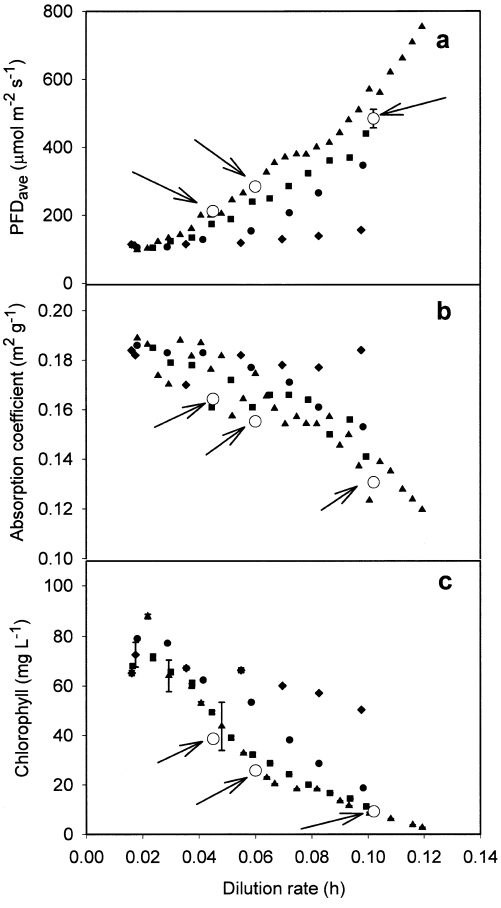

Figure 5. Effect of acceleration rates of 0.00809 h^{-2} (◆), 0.00107 h^{-2} (●), 0.00029 h^{-2} (■), and 0.00016 h^{-2} (▲) during A-stat cultivations on (a) average light intensity inside the reactor (PFD_{ave}), (b) specific absorption coefficient, and (c) chlorophyll concentration, and comparison to results obtained in chemostats (○) run at different dilution rates. Error bars represent standard errors for the A-stat data and 95% confidence interval for the chemostat data points.

A-Stat Versus Chemostat

To validate the A-stat, culture characteristics obtained with the A-stat run at different acceleration rates were compared with steady-state characteristics obtained from chemostat cultivations. This comparison was based on biomass concentration, average light intensity inside the reactor, absorption coefficient, and chlorophyll concentration (Figs. 4 and 5). It was clearly shown that, at low acceleration rates (0.00016 and 0.00029 h^{-2}), the culture characteristics in the A-stat are identical to those obtained in the chemostat at the same dilution rate. An increased acceleration rate generally resulted in increased deviation between the results from the A-stat and the chemostat.

Sluis et al. (2001) proved that these differences were dependent on both the delay of the concentrations of the medium components and the limitation in the metabolic adaptation rate of the microorganism, for yeast cultivations.

In this work, the delay in average light intensity during the A-stat was not directly due to a fast acceleration rate but rather to a delay in the decrease of biomass concentration at high acceleration rates (Fig 4).

At the highest acceleration rate (0.00809 h^{-2}), there were no changes in light intensity (Fig. 5a) and simulation [Eq. (9)], and experimental data at this acceleration rate (Fig. 4) showed good agreement. This implies that the experimental biomass concentration was only a function of the fast increase in dilution rate.

An acceleration rate of 0.00108 h^{-2} led to a small deviation between A-stat and chemostat (Figs. 4 and 5). This was due to the delay in the decrease in biomass concentration and not to a limitation in the metabolic adaptation of the microalgae. Figure 6 shows that the delay in the decrease of biomass concentration is eliminated by plotting the culture characteristics against the concentration of biomass instead of the dilution rate. There is no deviation between the specific growth rate and chlorophyll concentration in the A-stat (a = 0.00107 h^{-2}) and chemostat at the same dilution rate.

Optimization of Biomass and Product Yield on Light Energy

The predominant factor determining the biomass yield on light energy is the light regimen inside the reactor, which is characterized by: (1) light intensity at the reactor surface; (2) duration of exposure of individual cells to the photic and dark volumes of the reactors; and (3) the frequency of fluctuation between these volumes. In these experiments, both the incident light intensity and the frequency of fluctuation remained constant; only the percentage of photic and dark volumes changed during the A-stat and, consequently, the relative time that cells spent in the photic and dark zone of the reactor. The volumetric productivity and biomass yield on light energy obtained during the A-stat are shown in Figure 7. A plateau can be seen over a range of dilution rates (0.03 to 0.05 h^{-1}), where the volumetric productivity and the yield on light energy yield are maximal, 1.5 g L^{-1} day^{-1} and 0.6 g mol^{-1}, respectively. This range of dilution rates corresponds to a range of average light intensities ranging from 120 to 210 μmol m^{-2} s^{-1} and to a photic zone (a zone where 90% of the incoming light is absorbed) of 36% to 68% of the total reactor volume (Fig. 7). Apparently, the culture can utilize the light with the same efficiency within this range in this photobioreactor, with an incident light intensity of 1000 μmol m^{-2} s^{-1}. This plateau effect has been reported by Cornet et al. (1992) and Barbosa et al. (2003).

Excessive light absorption under high light intensities can cause photo-oxidative damage to the photosynthetic reaction centers (Casper-Lindley and Björkman, 1998). Photosynthetic organisms have developed mechanisms to safely dissipate excessive energy as heat (nonphotochemical quenching, or NPQ), and thus the energy arriving at the reaction centers decreases.

Dunaliella has a light-harvesting complex, containing chlorophyll a and b and β-carotene, lutein (α-carotenoid), and the β-carotenoid xanthophyll-cycle pigments violaxanthin, anteraxanthin, and zeaxanthin (Jansson, 1994). The β-carotenoid xanthophyll cycle pigments have the capacity to dissipate excess light energy as heat. Lutein has a structural function in the light-harvesting complex II (LHC II)

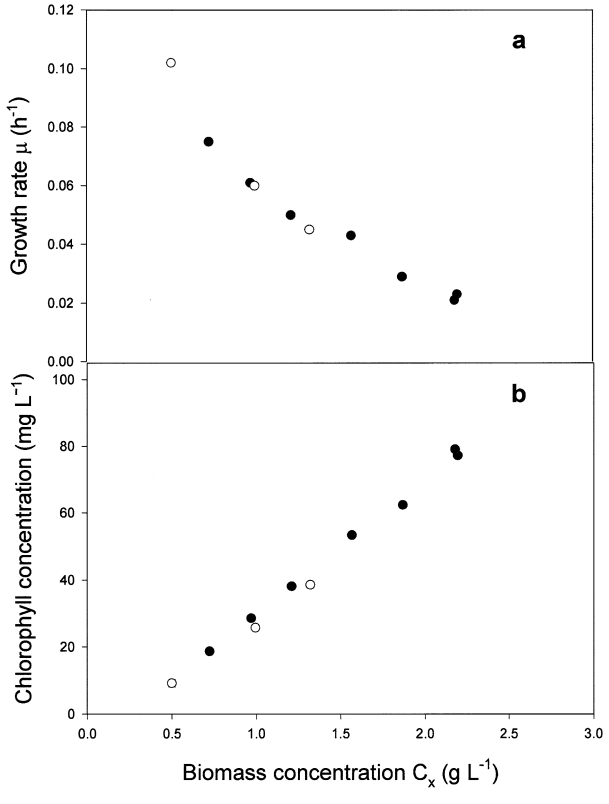

Figure 6. Effect of biomass concentration on (a) growth rate and (b) chlorophyll concentration during the A-stat performed at an acceleration rate of 0.00107 h^{-2} (●) and for the chemostats performed at three different dilution rates (○).

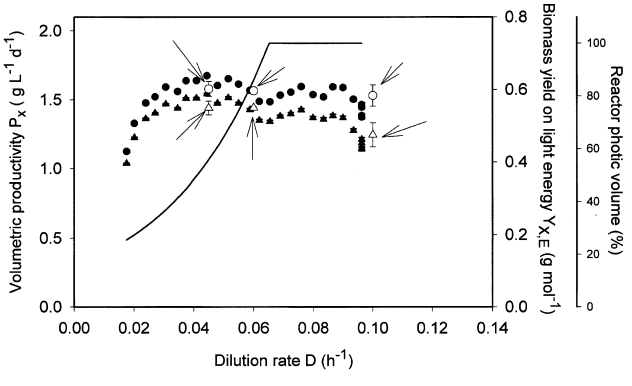

Figure 7. Effect of dilution rate on: (1) volumetric productivity (P_x) for the A-stat at an acceleration rate of 0.00015 h^{-2} (▲) and chemostat (△) experiments; (2) biomass yield on light energy ($Y_{x,E}$) for the A-stat at an acceleration rate of 0.00015 h^{-2} (●) and chemostat experiments (○); and (3) photic volume as a percentage of the total reactor volume (solid line). Error bars represent standard errors.

monomer and its energy-quenching effect has been reported (Green and Kühlbrandt, 1995). Chlorophylls and β-carotene are responsible for light absorption and β-carotene also works as an antioxidant in the protection against excessive light and as a precursor of the xanthophyll pigments (Phillips et al., 1995; Young et al., 1997).

Vitamins E (α-tocopherol) and C (ascorbic acid) are also present in *Dunaliella tertiolecta* (Abalde and Fabregas, 1991; Fabregas and Herrero, 1990) and they also have a protective role against photo-oxidation. Vitamin E works as a radical, trapping antioxidants with β-carotene (Palozza and Krinsky, 1992).

Vitamin C, besides acting as an antioxidant, can regenerate vitamin E after it has functioned as a radical-trapping antioxidant (Doba et al., 1985; Niki, 1987).

The optimization of product yield (vitamins C and E, lutein, and β-carotene) on light energy was carried out using the A-stat at an acceleration rate of 0.00015 h^{-2}. Figure 8 shows the volumetric productivities obtained during the A-stat, at different dilution rates.

Vitamin E (α-tocopherol) is the most active of the tocopherols, representing 96% and 80% of the total tocopherols at the beginning and end of the A-stat, respectively.

A significant negative correlation was found between the yield of vitamin E and the average light intensity (Spearman rank correlation coefficient = −0.680, data not shown).

Kusmic et al. (1999) observed an enhancement of vitamin E content in *Euglena gracilis* under an incident light intensity of 1000 μmol m^{-2} s^{-1}, by comparison with experimentation under dark conditions. Ogbonna et al. (1999) reported a simultaneous increase of α-tocopherol content in *E. gracilis* by decreasing the chlorophyll cell content. They kept the incident light intensity at 300 μmol m^{-2} s^{-1} and increased the biomass concentration. However, our results show the opposite tendency; the vitamin E yield on light energy decreased when increasing the average light intensity inside the reactor, as shown in Table I. The vitamin E cell content decreased from 0.33 ± 0.06 to 0.16 ± 0.03 mg g^{-1} (±95% confidence interval [CI]) by increasing the average light intensity from 84 ± 6 to 430 ± 34 μmol m^{-2} s^{-1} (±95% CI). *Dunaliella* and *Euglena* have different xantophyll cycle pigments; *Euglena* has been reported not to have xantophylls such as lutein (Casper-Lindley and Björkman, 1998) and *Dunaliella* contains large amounts of lutein, up to 5.65 ± 0.2 mg g^{-1} (Table I). It may also have a role in dissipation of excessive light. These two strains also have differing behavior toward the same light intensity, suggesting that they might have different photoprotective mechanisms.

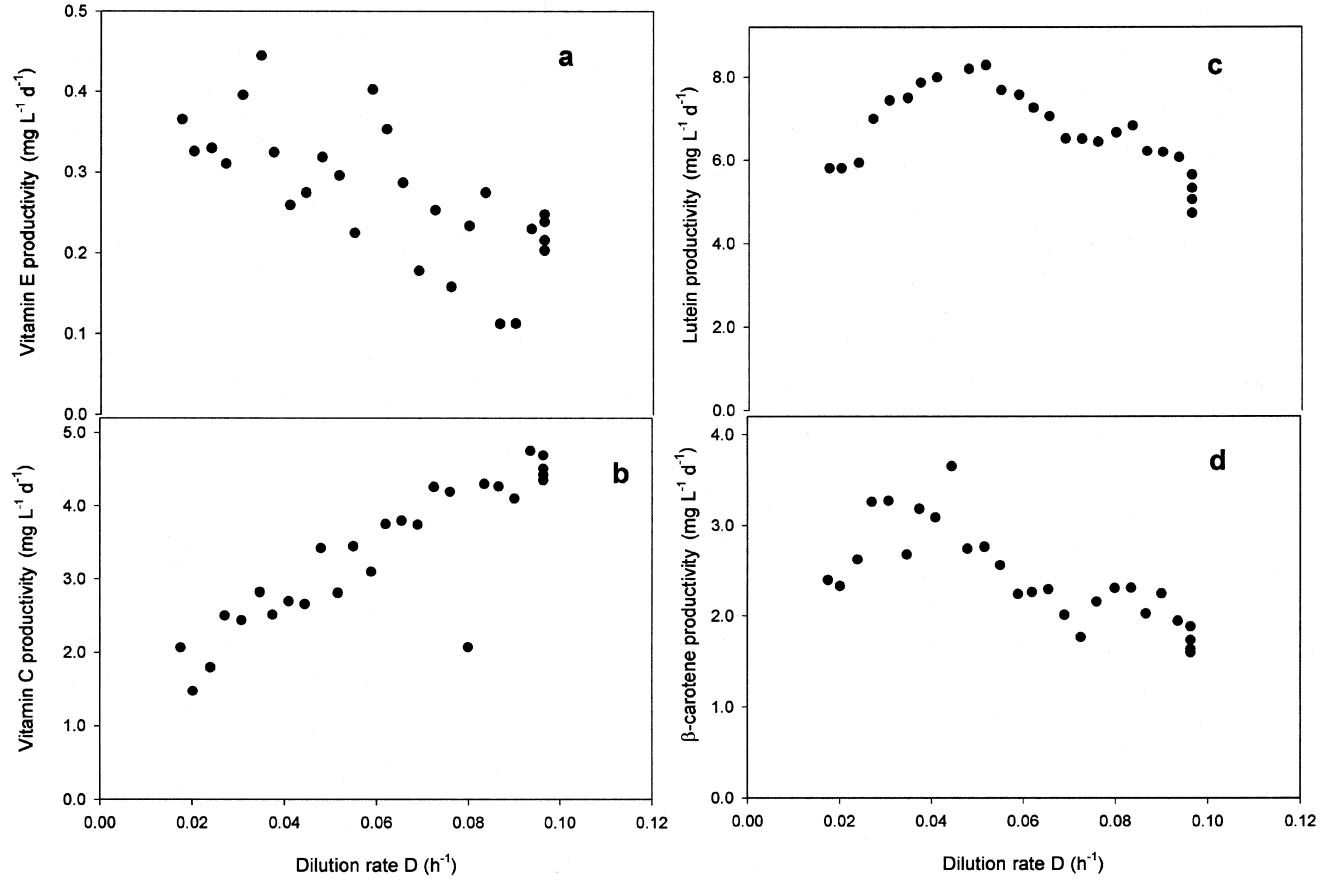

Figure 8. Effect of dilution rate on volumetric productivities of the products: (a) vitamin E; (b) vitamin C; (c) lutein; and (d) β-carotene. Results were obtained during the A-stat performed at an acceleration rate of 0.00015 h^{-2}.

Table I. Vitamin content of *D. tertiolecta* at the beginning and at the end of the A-stat (±95% CI).

	PFD_{ave} (84 ± 6 μmol m^{-2} s^{-1})	PFD_{ave} (430 ± 34 μmol m^{-2} s^{-1})
Biomass concentration (g L^{-1})	2.46 ± 0.07	0.51 ± 0.02
Dilution rate (h^{-1})	0.0175	0.096
Content per biomass (mg g^{-1})		
Vitamin E	0.33 ± 0.06	0.16 ± 0.03
Vitamin C	1.72 ± 0.76	3.48 ± 0.46
Lutein	5.65 ± 0.24	4.07 ± 0.13
β-carotene	2.36 ± 0.38	1.36 ± 0.01
Zeaxanthin	<0.005	<0.005

The biosynthesis of vitamin E in the cell is still not fully understood. Varied findings were obtained among the different studies; according to Threlfall and Goodwin (1967), most tocopherols in light-grown *Euglena* are synthesized inside the chloroplasts, with smaller amounts in mitochondria and microsomes. According to Shigeoka et al. (1986), most tocopherols of *Euglena* are synthesized inside the mitochondria, with smaller amounts in chloroplasts and microsomes, and the lowest amounts in cytosol. According to Tani and Tsumura (1989), nonphotosynthetic microorganisms do not produce detectable amounts of vitamin E. Kusmic et al. (1999) found indications that the formation of vitamin E occurs equally inside both mitochondrial and chloroplastic compartments, and that the correlation between light and vitamin E production is not linked to the existence of chlorophyll.

In this study, a clear correlation between chlorophyll and vitamin E contents of the cells was not observed. However, we found a negative correlation between the amount of vitamin E produced per mole of photons absorbed and the average light intensity inside the reactor. This finding makes vitamin E a promising compound for high-cell-density cultivations, where the average light intensity is always low (<100 μmol m^{-2} s^{-1}) and, consequently, the vitamin E cell content would be higher.

A clear increase in the vitamin C yield with increasing average light intensity was observed. The vitamin C content of the cells increased from 1.72 ± 0.76 to 3.48 ± 0.46 mg g^{-1} with increasing average light intensity from 84 ± 6 to 430 ± 34 μmol m^{-2} s^{-1} (Table I). The highest vitamin C content found in the present work (3.48 ± 0.46 mg g^{-1}) is higher than the values previously reported for *Dunaliella tertiolecta* (Abalde and Fabregas, 1991; Fabregas and Herrero, 1990), probably due to the use of higher light intensities in the present work.

The yield of lutein and β-carotene decreased slightly with increasing average light intensity inside the reactor. The biomass content of both carotenoids also decreased from 5.65 ± 0.24 to 4.07 ± 0.13 mg g^{-1} for lutein and from 2.36 ± 0.38 to 1.36 ± 0.01 mg g^{-1} for β-carotene with an increase of average light intensity from 84 ± 6 to 430 ± 34 μmol m^{-2} s^{-1} (Table I). Due to the antioxidative function of these carotenoids, the inverse behavior was expected; that is, an increase in the biomass content of both carotenoids with increasing light intensity. The amount of lutein per chlorophyll increased slightly and the amount of β-carotene per chlorophyll remained constant, which is in agreement with the work of Casper-Lindley and Björkman, (1998). They also reported that the amount of zeaxanthin per chlorophyll increased with increasing light intensity from 100 to 400 μmol m^{-2} s^{-1}, which indicates that zeaxanthin has an active role in the nonphotochemical quenching of light energy in *D. tertiolecta*. In the present work, the amount of zeaxanthin did not increase with increased light intensity from 84 ± 6 to 430 ± 34 μmol m^{-2} s^{-1} (Table I), which means that little or no light inhibition occurred during the A-stat.

In summary, the accuracy and reproducibility of the A-stat applied to microalgae cultures were studied. The fastest possible acceleration rate making it possible to achieve pseudo-steady-state culture conditions was 0.00029 h^{-2}. Rough estimations of steady-state culture characteristics can be made with an acceleration rate of 0.00107 h^{-2}. The results obtained using the A-stat at acceleration rates of 0.00016 and 0.00029 h^{-2} were similar to those obtained by the chemostats at the same dilution rates. It was shown that the A-stat is accurate and useful due to the shorter experimental time and increased quantity of information obtained. The A-stat was applied to optimize the biomass and product yield of *D. tertiolecta*. The effect of average light intensity on the cell content of vitamins C and E, lutein, and β-carotene was also studied. There was no correlation between the amount of vitamin E and chlorophyll in the cells. The cell content of vitamin E decreased, whereas the amount of vitamin C increased with increasing average light intensity. This makes vitamin E a promising compound for production with high-cell-density microalgae cultivations.

NOMENCLATURE

a	acceleration rate (h^{-2})
a_c	spectral-averaged absorption coefficient on a dry weight basis (m^2 g^{-1})
a_c (λ)	wavelength-dependent specific absorption coefficient (m^2 g^{-1} nm^{-1})
$b_{reactor}$	reactor light path (m)
C	concentration (g L^{-1})
D	dilution rate (h^{-1})
E_a	light absorbed by the culture (μmol photons s^{-1})
PFD	photon flux density (μmol m^{-2} s^{-1})
PFD (λ)	wavelength-dependent photon flux density (μmol m^{-2} s^{-1} nm^{-1})
P_x	biomass volumetric productivity (g L^{-1} day^{-1})
t	time (h)
μ	specific growth rate (h^{-1})
μ_{max}	maximum specific growth rate (h^{-1})
$V_{reactor}$	reactor volume (L)
$Y_{i,E}$	yield of component i on light energy (g mol^{-1})

$Y_{x,E}$	biomass yield on light energy (g mol^{-1})
λ	wavelength (nm)

Subscripts

x	biomass
vit E	vitamin E
vit C	vitamin C
0	initial
f	final
out	outgoing
in	ingoing
ave	average

References

Abalde J, Fabregas J. 1991. β-carotene, vitamin C and vitamin E content of the marine microalga *Dunaliella tertiolecta* cultured with different nitrogen sources. Biores Technol 38:121–125.

Abe K, Nishimura N, Hirano M. 1999. Simultaneous production of β-carotene, vitamin E and vitamin C by the aerial microalga *Trentepohlia aurea*. J Appl Phycol 11:331–336.

Barbosa MJ, Hoogakker J, Wijffels EH. 2003. Optimisation of cultivation parameters in photobioreactors for microalgae cultivation using the A-stat technique. Biomol Eng 20:115–123.

Broekmans WM, Berendschot TT, Klopping-Ketelaars IA, de Vries AJ, Goldbohm RA, Tijburg LB, Kardinaal AF, van Poppel G. 2002. Molecular pigment density in relation to serum and adipose tissue concentrations of lutein and serum concentrations of zeaxanthin. Am J Clin Nutr 76:595–603.

Casper-Lindley C, Björkman O. 1998. Fluorescence quenching in four unicellular algae with different light-harvesting and xantophyll-cycle pigments. Photosynth Res 56:277–289.

Cornet JF, Dussap CG, Cluzel P, Dubertret G. 1992. A structured model for simulation of cultures of the cyanobacterium *Spirulina platensis* in photobioreactors: II. Identification of kinetic parameters under light and mineral limitations. Biotechnol Bioeng 40:826–834.

Doba T, Burton GW, Ingold KU. 1985. Antioxidant and co-antioxidant activity of vitamin C. The effect of vitamin C, either alone or in the presence of vitamin E or water-soluble vitamin E analogue, upon the peroxidation of aqueous multilamellar phopholipid loposomes. Biochim Biophys Acta 835:298–303.

Falkowski PG, LaRoche J. 1991. Minireview: Acclimation to spectral irradiance in algae. J Phycol 27:8–14.

Fabregas J, Herrero C. 1990. Vitamin content of four marine microalgae. Potential use as source of vitamins in nutrition. J Indust Microbiol 5: 259–264.

Green B, Kühlbrandt W. 1995. Sequence conservation of light-harvesting and stress-response proteins in relation to the three-dimensional molecular structure of LHC II. Photosynth Res 44:139–148.

Jansson S. 1994. The light-harvesting chlorophyll *a/b*-binding proteins. Biochim Biophys Acta 1184:1–19.

Janssen M, Tramper J, Muur LR, Wijffels RH. 2002. Enclosed outdoor photobioreactors: light regime, photosynthetic efficiency, scale-up and future prospects. Biotechnol Bioeng 81:193–210.

Kusmic C, Barsacchi R, Barsanti L, Gualtieri P, Passarelli V. 1999. *Euglena gracilis* as source of the antioxidant vitamin E. Effect of culture conditions in the wild strain and in the natural mutant WZSL. J Appl Phycol 10:555–559.

Niki E. 1987. Interaction of ascorbate and α-tocopherol. Ann NY Acad Sci 498:186–199.

Ogbonna JC, Tomiyama S, Tanaka H. 1999. Production of α-tocopherol by sequential heterotrophic–photoautotrophic cultivation of *Euglena gracilis*. J Biotechnol 70:213–221.

Paalme T, Kahru A, Elken R, Vanatalu K, Tiisma K, Vilu R. 1995. The computer-controlled continuous culture of *Escherichia coli* with smooth change of dilution rate (A-stat). J Microbiol Meth 24: 145–153.

Palozza P, Krinsky NI. 1992. β-carotene and α-tocopherol are synergistic antioxidants. Arch Biochem Biophys 297:184–187.

Phillips LG, Cowan AK, Rose PD, Logie MRR. 1995. Operation of the xanthophyll cycle in non-stressed and stressed cells of *Dunaliella salina* Teod. in response to diurnal changes in incident irradiation: a correlation with intracellular β-carotene content. J Plant Physiol 146: 547–553.

Richmond A, Cheng-Wu Z. 2001. Optimization of a flat plate glass reactor for mass production of *Nannochloropsis* sp. outdoors. J Biotechnol 85:259–269.

Speek AJ, Schrijvers J, Schreurs WHP. 1984. Fluorimetric determination of total vitamin C and total vitamin iso-C in foodstuffs and beverages by high performance liquid chromatography with pre-column derivatization. J Agric Food Chem 32:352–355.

Speek AJ, Schrijvers J, Schreurs WHP. 1985. The vitamin E composition of some seed oils as determined by high performance liquid chromatography with fluorimetric detection. J Chromatogr 224:389–397.

Shigeoka S, Onishi T, Nakano Y, Kitaoka S. 1986. The contents and subcellular distribution of tocopherols in *Euglena gracilis*. Agric Biol Chem 50:1063–1065.

Sluis C, Westerink B, Dijkstal M, Castelein S, Boxtel A, Giuseppin M, Tramper J, Wijffels RH. 2001. Estimation of steady-state culture characteristics during acceleration-stats with yeasts. Biotechnol Bioeng 75: 267–275.

Tani Y, Tsumura H. 1989. Screening for tocopherol-producing microorganisms and α-tocopherol production by *Euglena gracilis* Z. Agric Biol Chem 53:305–312.

Takeyama H, Kanamaru A, Yoshino Y, Kakuta H, Kawamura Y, Matsunaga T. 1997. Production of antioxidant vitamins, β-carotene, vitamin C, and vitamin E, by two-step culture of *Euglena gracilis* Z. Biotechnol Bioeng 53:185–190.

Threlfall DR, Goodwin TW. 1967. Nature, intracellular distribution and formation of terpenoid quinones in *Euglena gracilis*. Biochem J 103: 573–588.

Young AJ, Orset S, Tsavalos AJ. 1997. Methods for carotenoid analysis. In: Pessarakli M, editor. Handbook of photosynthesis. New York: Marcel Dekker. p 575–596.